Sequence-dependent Guest Release Triggered by Orthogonal Chemical Signals

Ana M. Castilla, Tanya K. Ronson, and Jonathan R. Nitschke*

Department of Chemistry, University of Cambridge, Lensfield Road, Cambridge CB2 1EW, United Kingdom

Supporting Information Placeholder

ABSTRACT: Three $Zn^{II}_4L_4$ coordination cages, assembled from *tris*-iminopyridine ligands, exhibit differences in their guest-binding selectivities and reactivity with tris(2-aminoethyl)amine (*tren*), which enabled the design of a molecular network that responded in distinct ways to different chemical signals. When two of these cages were present in solution together, one of them was observed to selectively encapsulate chloroform, and the other, cyclohexane. The two guests could be released sequentially, in a specified order defined by the input of two separate chemical signals: *tren* and perrhenate. Furthermore, the observed reactivity of *tren* with the initial cage mixture provided control over the uptake and release of perrhenate within the third cage formed *in situ*. One of these tetrahedral cages has been identified as a tight ($K_a > 10^7$ M^{-1}) and selective host for perrhenate, an anion of great physicochemical similarity to pertechnetate, both having uses in nuclear medicine.

Introduction

Increasingly fine control over the processes and outcomes of chemical self-assembly has enabled the development, in recent years, of complex *chemical systems* with useful functions that emerge from the collectivity of their individual components.[1,2] In order to shape these functions, studies have been carried out into designing molecular networks and elucidating how they behave in response to stimuli.[3] These synthetic chemical networks enable the design of materials able to adapt their properties to changes in the environment.[3a-g,4] Advances in this area require gaining control over systems in which different stimuli trigger independent and distinct responses, allowing different behavior to be engendered.[5,6] Selective sequences of stimuli have been employed to determine the direction of travel of a molecular walker[5b] or the successive release of cargos from silica nanoparticles.[5c]

The well-defined inner phases of self-assembled metal-organic polyhedra[7,8] have proven useful in a diverse range of applications,[9] from molecular recognition and sensing[8a,10] to gas sequestration,[11] stabilization of reactive species[12] and catalysis.[13] These hosts are excellent candidates for incorporation into molecular networks to explore complex and stimuli-responsive behaviors[14,15] due to their encapsulation abilities and the dynamic nature of the linkages that hold them together. Investigating systems that comprise multiple hosts and guests together may allow for new functions to be designed, beyond what is achievable with single host-guest systems.[14a,15c,16]

Here we describe a system composed of self-assembled cages that has been designed to exhibit complex guest release behavior in response to two distinct chemical signals. These are a competing guest and a reagent, *tren*, which effects a host transformation. In addition, we demonstrate the system's overall response to be dependent on the sequence of applied stimuli, a property that is not characteristic of any one cage structure, but which emerges from the system. This sequence dependent response confers a further level of complexity on the system, which would not be attainable by a simple collection of two receptors that bind two different guests, where release can be triggered by the addition of other competing guests for example.

Results and Discussion

To design this system, we selected three face-capped[17] $Zn^{II}_4L_4$ tetrahedral capsules, in which tritopic iminopyridine ligands are formed from either a phenyl-centered tris-aniline[16c,17a] or a phenyl-centered tris-formylpyridine.[18] A detailed study allowed us to identify two key features for the implementation of a stimuli-responsive molecular network: First, contrasting guest binding preferences and affinities, and second, orthogonal reactivities of the tris-aniline and tris-formylpyridine based structures with tris(2-aminoethyl)amine (*tren*). Consideration of these features led to the design of the network depicted in Scheme 1. Two different neutral guests, cyclohexane and chloroform were each selectively encapsulated in one of the two $Zn^{II}_4L_4$ hosts (**1** - **2**). Each guest could be selectively released using one of two distinct chemical signals: treatment with *tren* released cyclohexane, and addition of perrhenate liberated chloroform. Reversing the order of the signals reversed the order of guest release. Intriguingly, whereas one signaling pattern (sequence I) resulted in complete destruction of the cages and ultimately ejection of perrhenate into solution, the reverse pattern (sequence II) allowed perrhenate to be trapped within a stable host (**3**) formed at the end of the sequence.

The design of this network is grounded upon systematic investigations of the guest binding properties of hosts **1**-**3** (Scheme 1), which also revealed the unprecedented affinity of new hosts **2** - **3** for perrhenate.[19,20] This anion is relevant as a surrogate in the design of receptors for radioactive pertechnetate, and also to applications in nuclear medicine; the development of selective perrhenate and pertechnetate receptors has proven particularly challenging.[19,21] Furthermore, the significant differences in anion uptake kinetics were uncovered between tris-formylpyridine-based cages **2** and **3**, whose vertices are capped with three toluidine residues or one *tren*, respectively. These differences provided insight into the guest uptake and exchange mechanisms[22] of the face-capped tetrahedra described herein.

Scheme 1. Sequence-Selective Release of Guests Triggered by Orthogonal Chemical Signals.[a]

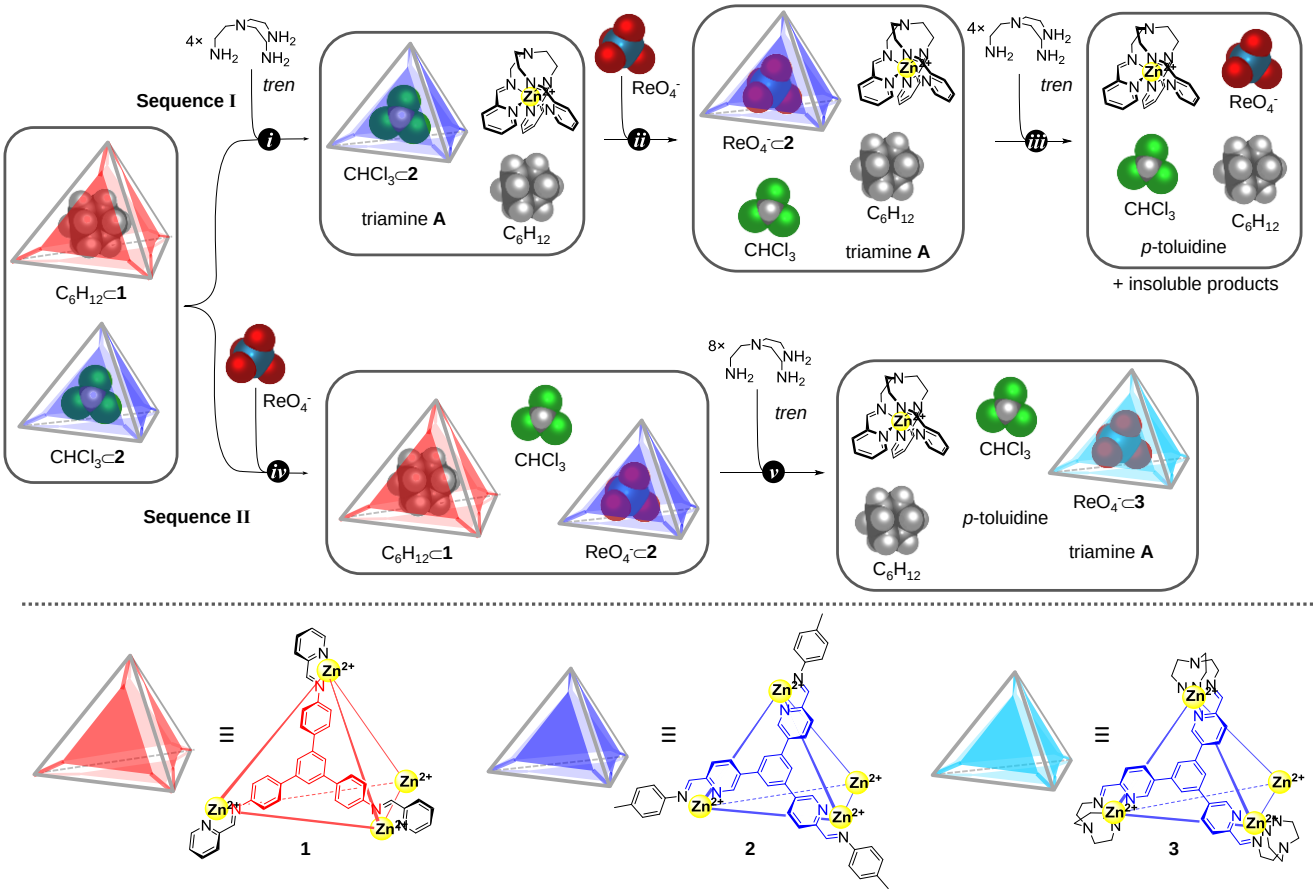

[a]**Signal Sequence I:** *i*) disassembly of **1** and release of C_6H_{12}; *ii*) release of $CHCl_3$ by displacement with ReO_4^- from the cavity of **2**; *iii*) release of ReO_4^- upon disassembly of **2**. **Signal sequence II**: *iv*) release of $CHCl_3$ by displacement with ReO_4^- from the cavity of **2**; *v*) simultaneous breakdown of **1** releasing C_6H_{12} and transformation of **2** into **3** while maintaining sequestration of ReO_4^-. **A** and **B** denote the face-capping subcomponents 1,3,5-tris(4'-aminophenyl)benzene (for cage **1**) and 1,3,5-tris(2'-formylpyridyl-5')benzene (for cages **2** - **3**). N.B. The insoluble products in Sequence I contain triamine **A** and trialdehyde **B**.

Synthesis and characterization of cages 1-3. Tetrahedra **1**-**3** (Scheme 2) self-assembled from zinc(II) and tritopic subcomponents: either 1,3,5-tris(4'-aminophenyl)benzene, **A**[17a] (cage **1**) or 1,3,5-tris(2'-formylpyridyl-5')benzene, **B**[18] (cages **2** and **3**). The synthesis if **1** has been previously described.[16c] The reaction of **B**, *p*-toluidine and zinc(II) bis(trifluoromethylsulfonyl)imide (triflimide, NTf_2^-) in a 1:3:1 ratio in acetonitrile afforded **2**, isolable as a greenish crystalline solid. Vapor diffusion of diethyl ether into an acetonitrile solution of **2** produced crystals suitable for analysis by single-crystal X-ray diffraction (Figure 1). The four facially coordinated Zn^{II} centers are bridged by four face-capping ligands, resulting in a tetrahedral arrangement with approximate *T*-symmetry. All Zn^{II} stereocenters within a cage share the same Δ or Λ stereochemistry; both cage enantiomers are present in the crystal. The cavity of **2** is almost completely enclosed by the ligands, with pores of less than 1.3 Å in diameter. The Zn-Zn distances are in the range 11.278(4)-11.774(3) Å (average 11.5 Å) and the cavity volume was calculated to be 130 $Å^3$ using VOIDOO (see section 7 in the Supporting Information).[23]

Similarly, the reaction in acetonitrile/methanol (1:1) of **B**, *tren* and $Zn(NTf_2)_2$ in a 1:1:1 ratio generated tetrahedral cage **3**, isolable as a yellowish crystalline solid. The single-crystal structure of **3** (Figure 1) closely resembles that of **2**, except that *tren* residues cap the vertices of the tetrahedron, forming an extended cryptand-like architecture. The Zn-Zn distances of 11.749(3)-11.775(3) Å fall within the range observed for **2**;

the average distance is 11.8 Å. The cavity volume was calculated to be 111 Å^3, marginally smaller than **2** due to the faces of **3** pressing inward slightly relative to those of **2** (see section 7 in the SI). The use of a smaller tris-formylpyridine based ligand thus leads to cages that enclose less volume than cage **1** (Zn-Zn distance 14.6 Å, volume 188 Å^3), formed from the analogous tris-aniline subcomponent **A** (Figure 1).[16c]

Scheme 2. Subcomponent Self-Assembly of cages 1 - 3 and the transformation of 2 into 3.[a]

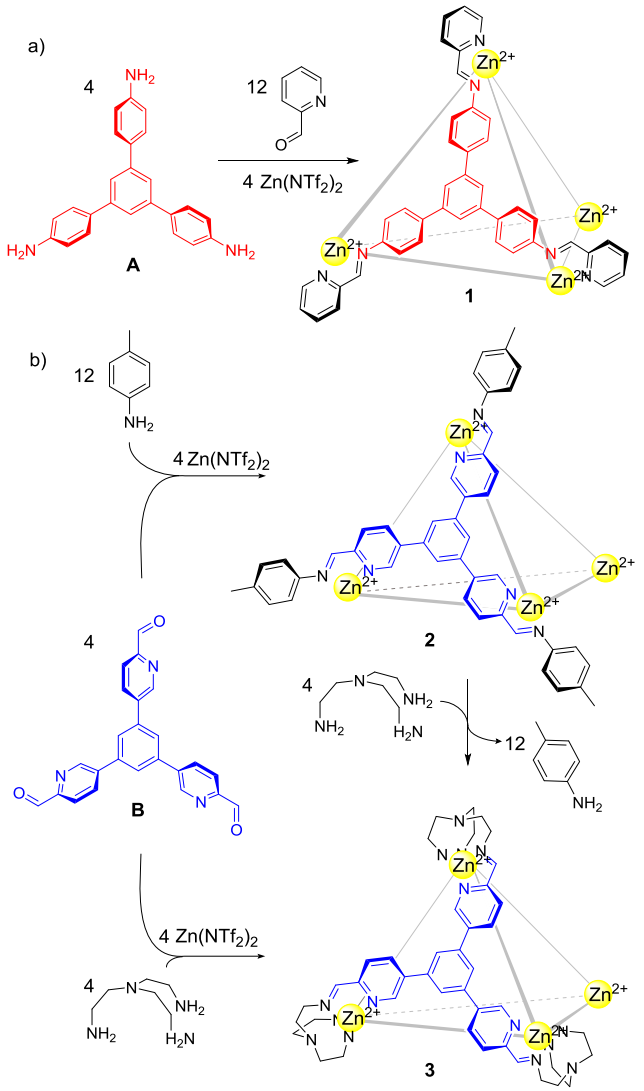

[a]Only one ligand is drawn per structure for clarity.

ESI-MS and NMR analyses reflect solution structures of **2** and **3** analogous to what is observed in the solid state. Their simple ^{1}H NMR spectra, with only one set of ligand resonances, are consistent with the formation of a single diastereomer with *T* point symmetry. Their ^{19}F NMR spectra, with only one sharp signal having a chemical shift corresponding to unencapsulated NTf_2^-, confirmed that the cages do not bind this anion in solution (Figures S3 - S4). Triflimide was, indeed, chosen specifically to avoid counterion encapsulation, in order to facilitate host-guest studies.[10a] Considering the volumes of their Fe^{II}-templated analogs,[18] we anticipated that NTf_2^- (157 Å^3) would be too voluminous to fit in the cavity of cages **2** and **3**.[10a]

In similar fashion to their Fe^{II}-containing congeners,[18] cage **3** could also be prepared through substitution of the twelve *p*-toluidine residues incorporated into the periphery of cage **2** with four equivalents of *tren* (Scheme 2). The treatment of a solution of cage **2** in acetonitrile with 4.5 equivalents of *tren* at 70 ºC afforded cage **3** as the only product observed by ^{1}H NMR and ESI-MS (see section 4.4 in the SI). We infer this imine exchange reaction to be driven by the more electron-rich character of *tren* and the chelate effect.

Cage **2** was also prepared from the zinc(II) salts of tetrafluoroborate (**2**·$[BF_4]_8$), perchlorate (**2**·$[ClO_4]_8$) and triflate (**2**·$[OTf]_8$). Similarly **3**·$[OTf]_8$ was obtained from $Zn(OTf)_2$ in a CH_3CN/CH_3OH mixture. In contrast, attempts to form cage **3** from $Zn(BF_4)_2$ or $Zn(ClO_4)_2$ resulted in insoluble products. Cage **3**·$[BF_4]_8$ could, however, be prepared through reaction of **2**·$[BF_4]_8$ with *tren*, whereas analogous reactions with **2**·$[ClO_4]_8$ and **2**·$[OTf]_8$ afforded intractable precipitates.

Anion binding studies. The anion encapsulation abilities of cages **2** and **3** were probed by treating them in solution with a series of anions having different shapes and volumes (listed in tables S2 and S6 in the Supporting Information). Previous studies determined that tetrahedron **1** does not bind anions in its cavity.[16c,17a] Cage **2** was observed to bind the anions (in order of size) NO_3^-, BF_4^-, ClO_4^-, ReO_4^-, PF_6^-, SbF_6^- and TfO^-, as confirmed by ^{1}H and ^{19}F NMR. The addition of the tetrabutylammonium salt of ClO_4^-, ReO_4^-, PF_6^- or TfO^-, or the potassium salt of SbF_6^- (0.5 equiv) to a solution of **2**·$[NTf_2]_8$ resulted in the appearance of a new set of ^{1}H NMR signals, assigned to the inclusion complexes in slow exchange with the free cage on the NMR timescale (Figure S12). Solutions containing PF_6^- or TfO^- each showed two new ^{19}F NMR signals (in addition to the NTf_2^- resonance) attributed to free and encapsulated anions (Figures S8 and S15). The ^{19}F NMR spectrum of the solution containing SbF_6^- showed a broadened, extended multiplet assigned to this anion due to overlapping signals of free and encapsulated species.

In contrast, the addition of tetrabutylammonium salts of the smaller anions BF_4^- or NO_3^- to a solution of 'empty' **2**, provided evidence for anion binding in fast exchange. The ^{1}H NMR signals of the host were observed to shift, with the resonances due to the central phenyl and inward-facing pyridine protons undergoing the greatest shifts (Figure S12). In the case of BF_4^-, broadening of the ^{1}H and ^{19}F NMR spectra was also observed. Encapsulation of BF_4^- was further supported by a ^{1}H-^{19}F HOESY spectrum, in which correlations were observed between the anion resonance and signals corresponding to the protons of the ligand pointing towards the inside of the cavity (Figure S18). Other anions screened, such as Cl^-, Br^- or I^-, gave rise to a color change and precipitation following their addition to a solution of **2**·$[NTf_2]_8$, consistent with cage decomposition.

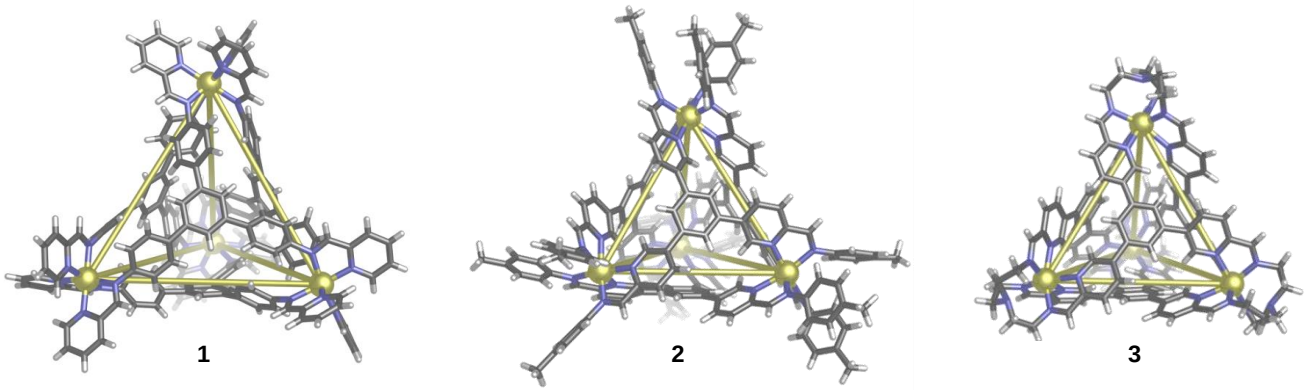

Figure 1. X-ray crystal structures of cages **1**,[16c] **2** and **3**. Anions and solvent molecules are omitted for clarity.

Anion-binding strengths were quantified through ^{1}H NMR titrations, and the results are given in Table 1 (see section 2.2 in the SI for experimental details). The affinity of **2** for SbF_6^-, ReO_4^- or TfO^- was found to be too high for an accurate direct determination of their K_a values, which were instead derived through competitive binding experiments: titration of SbF_6^- and TfO^- against $PF_6^-\subset$**2** and titration of ReO_4^- against $TfO^-\subset$**2** (Figure 2).

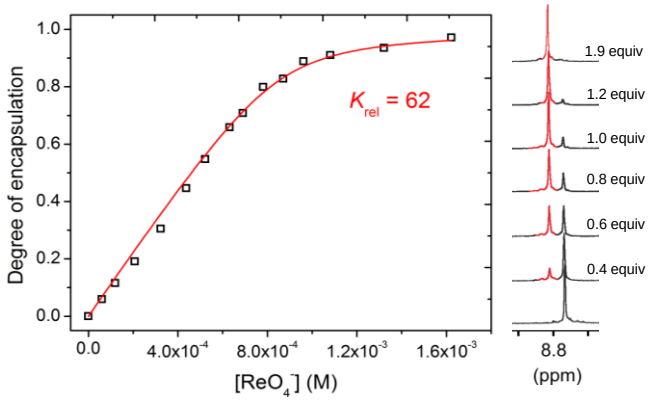

Figure 2. Left: Curve fit for the ^{1}H NMR titration of ReO_4^- into a solution of $TfO^-\subset$**2** in CD_3CN to a competitive binding model.[10a] Right: Imine region of selected ^{1}H NMR spectra showing formation of $ReO_4^-\subset$**2** (red) and consumption of $TfO^-\subset$**2** (black) upon addition of increasing amounts of ReO_4^-. See Figure S27 for further details on the data fitting.

In combination, these experiments show that cage **2** is capable of accommodating in its interior monocharged anions with volumes ranging from 40 to 85 Å^3 with the following hierarchy: $ReO_4^- > SbF_6^- > TfO^- > PF_6^- \approx NO_3^- > ClO_4^- > BF_4^-$. These relative affinities deviate from what would be predicted from Rebek's 55% occupancy optimum.[24,25] We infer that a subtle interplay of size and shape complementarities between host cavity and guest, solvation effects and electrostatic interactions determine together the observed hierarchy, with no single factor predominating.[20,26] Within a series of anions with the same geometry, larger anions are more strongly bound, such as ReO_4^- and SbF_6^-. Despite TfO^- and SbF_6^- having the same molecular volume (Table 1), we infer the better symmetry match between octahedral SbF_6^- and the tetrahedral cavity renders it a better guest. The high association constant determined for the trigonal planar NO_3^-, five times greater than that of the larger tetrahedral ClO_4^-, may be attributed to the lower hydrophobicity of nitrate.[27,20]

Table 1. Summary of binding constants (K_a) for anions in cages **2** and **3**.[a]

		K_a (M^{-1})[b] / NMR exchange	
Guest[c]	V (Å^3)[d]	**2**	**3**
NO_3^-	40.7	1.5(±0.3)×10^4 / fast	nonbinding
BF_4^-	53.3	7.1(±0.2)×10^2 / fast	nonbinding
ClO_4^-	54.8	3.0(±0.2)×10^3 / slow	nonbinding
ReO_4^-	59.8	2.2(±0.4)×10^7 / slow	>10^5 / slow
PF_6^-	74.7	1.4(±0.1)×10^4 / slow	21±3[e] / slow[f]
SbF_6^-	84.7	2.5(±0.6)×10^6 / slow	115±8[e] / slow[f]
TfO^-	85.0	3.6(±0.3)×10^5 / slow	41±3[e]/ no exchange observed

[a]Cage **1** does not encapsulate anionic guests.[16c,17a] [b]Full details of how K_a values and corresponding errors were calculated are given in the Supporting Information sections 2.2 and 2.3. [c]Addition of Cl^-, Br^-, or I^- to solutions of **2** or **3** induced cage decomposition. [d]Calculated *van* der Waals volumes, see the Supporting Information. [e]Estimated values. [f]Not observed below 70 ºC.

Strikingly, cage **3** was found to exhibit substantially different guest binding abilities from cage **2**, despite their structural similarities.[29] The addition of NO_3^-, BF_4^-, ClO_4^-, PF_6^- or TfO^- to a solution of **2**·$[NTf_2]_8$ in acetonitrile caused only slight (< 0.08 ppm) shifts in the ^{1}H NMR spectra, even after equilibration at room temperature for several hours (see Figures S33 and S47), in marked contrast with the behavior of the cage **2**. We attribute these changes to a weak interaction of the anions with the exterior of the cage rather than encapsulation.[30]

Previous work has shown that the incorporation of electron-rich or electron-poor aniline residues into the periphery of related $Fe^{II}_4L_6$ capsules did not affect their anion-binding preferences.[10a] We had therefore not anticipated that the exchange of *p*-toluidine for the more electron-rich *tren*, in going from **2** to **3**, would have such an impact on the anion-binding preferences. We reasoned the different behavior of

cage **3** may be attributed to the covalent locking effect of *tren* preventing partial cage opening during anion exchange (discussed below).[18,10h]

In order to probe whether the failure to observe anion binding within **3** is due to a thermodynamic or a kinetic effect, we performed three different sets of experiments followed by NMR, illustrated in Scheme 3. In the first (Scheme 3*i*), cage **3** was prepared from subcomponents in the presence of different prospective anionic guests. In the second (Scheme 3*ii*), the fates of anions encapsulated within **2** were charted during the course of a **2** to **3** transformation. In the third (Scheme 3*iii*), preformed **3**·$[NTf_2]_8$ was treated with the same series of anions at 70 ºC during a time course of many days. Cage **3** was observed to bind ReO_4^-, PF_6^-, SbF_6^- and TfO^-, but not NO_3^-, BF_4^-, or ClO_4^- during its formation (Scheme 3*i* & *ii*); the same set of anions were encapsulated following prolonged heating (Scheme 3*iii*), with the exception of triflate. Experimental details of anion encapsulation studies are provided in the Supporting Information section 2.3.

Scheme 3. Experiments probing the anion-binding properties of cage 3.[a]

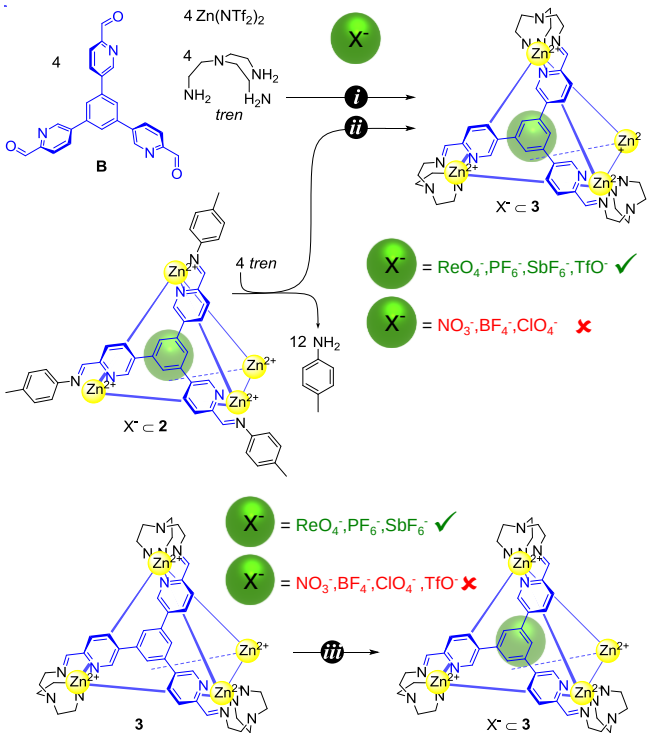

[a] *i)* When formed from subcomponents, **3** is observed to encapsulate ReO_4^-, PF_6^-, SbF_6^- and TfO^-, but not NO_3^-, BF_4^-, or ClO_4^-; *ii)* the same anion selectivity was observed during the formation of **3** from **2**; *iii*) the same anions were observed to be taken up within **3** following lengthy equilibration, except triflate.

Binding of perrhenate inside tetrahedron **3** was confirmed by X-ray crystallography (Figure 3). The encapsulated ReO_4^- is located close to the center of the tetrahedral cavity with the oxygen atoms oriented towards the zinc centers. The Zn-Zn distances and volume are similar to the empty cage. In addition, the complex $ReO_4^-\subset$**3** was found to be stable in water. The nitrate salt of the host-guest complex, although of modest solubility (ca. 0.2 mM), showed no degradation following 24 h at room temperature in D_2O (Figure S41).

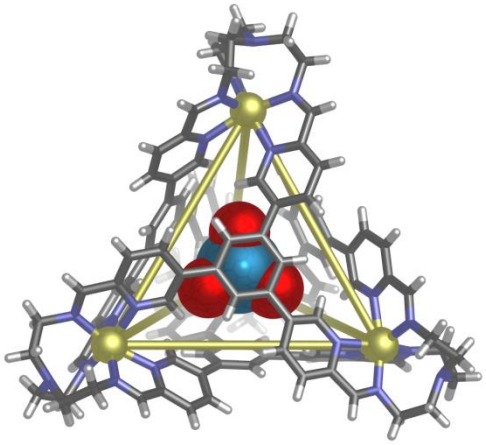

Figure 3. The crystal structure of $ReO_4^-\subset$**3**. Only one of the two crystallographically distinct cages is shown. The encapsulated ReO_4^- is shown in space-filling mode and non-encapsulated anions are omitted for clarity.

The slow uptake of anions into tetrahedron **3** prevented determination of their association constants through titration experiments. The binding strengths of PF_6^-, SbF_6^- and TfO^- were estimated by measuring the relative integration of signals due to free and bound host in the ^{1}H NMR spectra of samples following the transformation of **2** into **3** in the presence of an excess of the selected anion (Table 1). The binding of ReO_4^- to **3** was found to be too strong for estimation of its association constant by this method, but a lower limit of 10^5 M^{-1} could be obtained by NMR (see Supporting Information section 2.3.3).

In summary, with the exception of BF_4^-, NO_3^- and ClO_4^- which have been found to bind only to **2**, both tris-formylpyridine-based $Zn^{II}{}_4L_4$ structures **2** and **3** showed similar trends in anion-binding preferences: ReO_4^- >> SbF_6^- > TfO^- > PF_6^-.

The quantification of anion-binding strengths revealed an outstanding selectivity of cages **2** and **3** for ReO_4^-. Cage **2** has 10 and 60 times greater affinity for ReO_4^- than for SbF_6^- or TfO^-, respectively, the next most strongly bound anions (Table 1). As discussed above, this is likely due to a combination of symmetry match between host and guest and optimal volume occupation ratio. To the best of our knowledge, cage **2** represents the strongest 1 : 1 perrhenate binding host (K_a = 2.2±0.4 × 10^7 M^{-1}) reported to date in either organic or aqueous media.[19,21] The combination of water stability and exceptional affinity for ReO_4^- suggests that **3** might show promise in pertechnetate binding, of relevance in the context of radiopharmaceuticals and nuclear waste treatment, as discussed in the Supporting Information section 2.3.4.[19,20,21c,28]

Kinetics and mechanism of anion uptake. Despite showing similar anion binding preferences, very different guest exchange kinetics were observed for cages **2** and **3**. This observation led us to carry out a brief kinetic study, the results of which shed light upon the mechanisms of guest exchange. The smallest anions, NO_3^- and BF_4^-, exchanged between free and encapsulated states within **2** at a rate more rapid than the

NMR time scale. We estimate a lower limit of 30 s^{-1}, considering a difference of about 27 Hz between ^{1}H NMR resonances of the empty and guest-containing cage.[31] The guest exchange kinetics of ClO_4^- were examined by ^{1}H-^{1}H exchange spectroscopy (EXSY) NMR,[22b,32,33] providing an uptake rate constant (k_{in}) of $(3.0 \pm 0.5) \times 10^3$ $M^{-1}s^{-1}$, at 25 ºC. Rate constants for the guest exchange of ReO_4^-, PF_6^-, SbF_6^- and TfO^- could not be determined by EXSY because the uptake rates were too slow for the timescale of this technique (even at 70 ºC), but also too fast to be followed by ^{1}H NMR: in all cases the system had already reached equilibrium by the time the first ^{1}H NMR spectrum could be acquired following addition of anion to the cage solution. Considering the timescale of the EXSY experiment, we infer the k_{in} values for these guests to be lower than 10^3 $M^{-1}s^{-1}$ (see Supporting Information section 2.4 and Table S7).

The slower anion uptake rates exhibited by the *tren*-containing tetrahedron **3** allowed encapsulation to be followed by ^{1}H NMR (PF_6^-) or UV-vis (ReO_4^-), following the addition of excess anion to a solution of empty cage under *pseudo*-first order conditions. These experiments were performed at 70 ºC since exchange of PF_6^- was not observed at lower temperatures. At concentrations suitable for NMR analysis, the addition of any excess of ReO_4^- to **3** in solution caused precipitation. To circumvent this practical problem we followed ReO_4^- uptake at lower concentrations by UV-vis. The second-order rate constants k_{in} for ReO_4^- and PF_6^- were determined to be 47 ± 2 $M^{-1}s^{-1}$ and $1.7\pm0.4 \times 10^{-3}$ $M^{-1}s^{-1}$, respectively, at 70 ºC. The kinetics of inclusion for SbF_6^- and TfO^- into **3** could not be determined because of their very slow and non-observed uptakes, respectively (see section 2.4.2 in the SI).

The timescales for anion exchange given in Figure 4 illustrate the large differences in uptake rates between **2** and **3**. The incorporation of chelating *tren* in **3** was observed to slow encapsulation dramatically. Both of the plausible anion uptake mechanisms, diffusion of guest through the structure's portals, or partial disassembly to create transient larger portals,[22b] are expected to be more energetically costly in cage **3**. The covalent bonds of **3** must be distorted or cleaved in order for the cage to open, whereas **2** may be opened through the stretching or rupture of weaker coordinative linkages.

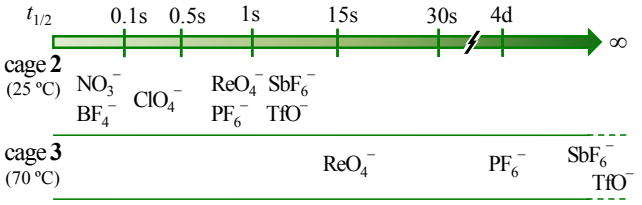

Figure 4. Relative timescales of anion uptake by cages **2** and **3**. Half-lives are based on apparent rate constants at a 1 mM guest concentration. N.B. For PF_6^- and **3**, no exchange was observed below 70 ºC.

The enclosed and rigid structure of the face-capped tetrahedra **2** - **3**, which appeared to leave no access for guest diffusion through the small portals on the edges (Figures S95 – S96), led us to hypothesize that the exchange of any guest would require N→Zn bond breakage. The observed marked dependence of anion uptake rates upon the size and shape of the guest, however, suggests that more than one mechanism may be at work. The fast exchange of the smallest anions BF_4^- and NO_3^- in and out of cage **2** seems unlikely to involve bond-breaking.[34] We infer that these anions may be undergoing exchange *via* a through-portal mechanism, whereby the ligands distort sufficiently to allow anion exchange without coordinative bond cleavage.[35,15b] The slower exchange exhibited by the largest anions PF_6^-, SbF_6^-, and TfO^- appears likely to involve partial cage opening and N→Zn bond rupture, which we infer to incur a considerably higher energetic penalty for cage **3**.[22b] Perchlorate, showing an uptake rate intermediate between these two classes of anions, may exchange *via* a more energetically-costly cage deformation, or partial vertex decoordination, or both. In addition, the higher association constants of ClO_4^- and ReO_4^-, having the same shape and slightly larger volumes than BF_4^-, can also hamper exchange, accounting for why the observed exchange timescale for ReO_4^- is on the same order as for the larger anions.

Collectively, the insights gained from these anion binding studies enables the design of systems incorporating the responsive behavior of tris-formylpyridine based cages **2** and **3** and anions: Guest release on treatment of an anion⊂**2** complex with an anion with higher affinity and treatment with *tren* to form **3** (Scheme 3*ii*) with concomitant guest release (NO_3^-, BF_4^- and ClO_4^-) or guest trapping in its cavity (ReO_4^-, PF_6^-, SbF_6^- and TfO^-).

Neutral guest binding. The ability of tetrahedral cages **1** - **3** to act as hosts for neutral molecules was also investigated in solution by NMR. To first establish the scope of guest binding we screened a series of neutral molecules, listed in Table 2, selected with different sizes and molecular volumes, distributed around the optimal guest volume for each cage predicted using Rebek's 55% optimum occupancy rule.[24] In all cases where host-guest complexes were inferred to form, the ^{1}H NMR spectrum of an equilibrated mixture of an excess of the selected guest and the cage in CD_3CN showed two sets of host peaks —attributed to empty $Zn^{II}_4L_4$ and guest⊂$Zn^{II}_4L_4$ in slow exchange— and also two sets of signals for the guest — assigned to the free and encapsulated guests (Figures S64 – S80).

Host **1** was reported in a preliminary study to accommodate cyclohexane and *t*BuOH within its cavity.[16c] We screened an extended series of neutral molecules, including those observed to bind inside cage **2** (see below), and also explored their relative binding strengths. The association constant (K_a) of cyclohexane in **1** was calculated through a ^{1}H NMR titration experiment to be $4.9\pm0.3 \times 10^2$ M^{-1}. For all other guests, affinities relative to cyclohexane were obtained by NMR on the basis of their ability to displace cyclohexane from the cavity of cage **1** (Supporting Information section 2.5.1). Host **1** was thus revealed to show similar guest-binding abilities to those of its Fe^{II} congener,[17a] although **1** was able to bind larger guests than the latter, such as cyclooctane and adamantane, due to its larger cavity.[17a,16c] The most strongly bound guests for **1** are CCl_4 > norbornane > norbornene > cyclopentane > cyclohexane.

Table 2. Comparison of neutral guest-binding properties of cages 1 and 2.[a]

		K_a (M^{-1})[b]	
Guest	V ($Å^3$)[c]	**1**[d]	**2**
CH_2Cl_2	60.9	low[e]	1.2(±0.2)
$CHCl_3$	74.7	$1.5(\pm0.1)\times10^2$	11(±0.2)
CCl_4	88.7	$1.2(\pm0.1)\times10^3$	15(±3)
*t*BuOH	95.4	low[e]	3.5(±0.8)
cyclopentane	95.3	$6.7(\pm0.4)\times10^2$	10(±0.8)
cyclopentanol	102.6	low[e]	6.6(±0.6)
methylcyclopentane	113.2	$1.6(\pm0.1)\times10^2$	2.8(±0.4)
1-methylcyclopentanol	120.5	low[e]	nonbinding
cyclohexane	111.9	$4.9(\pm0.1)\times10^2$[f]	nonbinding
norbornene	116.5	$6.9(\pm0.4)\times10^2$	6.8(±0.3)
norbornane	120.2	$1.1(\pm0.1)\times10^3$	5.2(±0.3)
7-bromonorbornane	138.3	49(±3)	nonbinding
cyclooctane	146.5	low[e]	[g]
benzene	99.5	low[e]	nonbinding
1,3,5-trifluorobenzene	113.1	nonbinding	nonbinding
1,3,5-trimethoxybenzene	180.1	nonbinding	nonbinding
naphthalene	151.0	nonbinding	nonbinding
n-pentane	106.8	low[e]	nonbinding
n-hexane	125.2	nonbinding	nonbinding
adamantane	159.1	59(±4)	[g]
1-bromoadamantane	177.3	nonbinding	[g]

[a]Cage **3** showed no evidence for binding neutral guests. [b]Full details of how K_a values and corresponding errors were calculated are given in Supporting Information section 2.5. [c]Calculated van der Waals volumes, see the Supporting Information for details. [d]From K_{rel} values determined in competitive experiments with cyclohexane. The reported error for each K_a value was estimated by error propagation analysis (see Table S8 and section 2.5.1). [e]Binding too weak to displace cyclohexane. [f]Determined by ^{1}H NMR titration. [g]Not examined for binding to **2** due to its large size

Host **2** was found to accommodate small hydrophobic molecules with volumes from 61 $Å^3$ (dichloromethane) to 120 $Å^3$ (norbornane). Notably, certain molecules, such as benzene, *n*-pentane or cyclohexane, with calculated volumes within the above range, did not bind within **2**, reflecting the necessity of a shape fit. In all cases the measured affinities were too weak to allow for determination of the binding constant *via* ^{1}H NMR titration. Instead, they were estimated by measuring the relative integration of signals for free and bound host in slow exchange at different guest concentrations (see section 2.5.1 in the Supporting Information). The strongest binders are CCl_4 > cyclopentane > $CHCl_3$, suggesting the volume range 75 – 95 $Å^3$ to be optimal for encapsulation within cage **2**.

None of the prospective neutral guests showed evidence for binding to cage **3**, even following heating to 60 ºC for 5 days, or assembly of **3** in the presence of excess prospective guest.

Selective guest binding within mixtures. Table 2 provides an overview of the neutral-guest-binding properties of tetrahedra **1** and **2**. From the data presented in Tables **1** and **2** it is possible to draw the following conclusions: *i*) tetrahedra **2** and **3** encapsulate anions with high affinities; *ii*) tetrahedron **3** binds a subset of the anions found to bind to **2**, with lower affinities; *iii*) **2** binds weakly a series of neutral molecules with volumes ranging 60-120 $Å^3$; *iv*) tetrahedron **1** encapsulates a wider range of neutral guests, including all of those observed to bind within **2**; *v*) in all cases **1** shows a higher affinity than **2** for each neutral guest, and for both cages the most strongly bound neutral guest is CCl_4. From these observations, several three-guest systems can be selected wherein two of the guests (C_6H_{12} and $CHCl_3$ in Scheme 1) are selectively bound to **1** and **2**, respectively, in a 1:1 cage mixture, and a third anionic guest (ReO_4^- in Scheme 1) may be added to the mixture in order to selectively trigger the release of the first guest from the cavity of cage **2**, thus acting as a selective chemical stimulus to the system.

Two sets of guests were selected to demonstrate sequence-selective release from an initial 1:1 mixture of **1**·$[NTf_2]_8$ and **2**·$[NTf_2]_8$ in CD_3CN. The first set of guests, shown in the system of Scheme 1, consists of the two neutral molecules C_6H_{12} and $CHCl_3$. The ^{1}H NMR spectrum after addition of C_6H_{12} and $CHCl_3$ (130 equiv each) showed selective binding of cyclohexane to **1** and of $CHCl_3$ to **2** (Figure S81). The subsequent addition of ReO_4^- (1.1 equiv) to the mixture showed selective formation of $ReO_4^-\subset$**2**.

The second set of guests comprises two anions (PF_6^- and ReO_4^-) and a neutral molecule (C_6H_{12}). ^{1}H and ^{19}F NMR spectra taken of a mixture of **1** (1 equiv), **2** (1 equiv), PF_6^- (1.7 equiv), and C_6H_{12} (88 equiv), showed exclusive formation of $C_6H_{12}\subset$**1** and $PF_6^-\subset$**2**. Subsequent addition of ReO_4^- (1.3 equiv) displaced PF_6^- from **2** to form the $ReO_4^-\subset$**2** complex (Figure S82).

Reaction of cage mixtures with *tren*. Next we set out to explore *tren* as a selective chemical stimulus, taking advantage of the differential reactivity of cages **1** and **2** towards this triamine. As discussed above, the reaction of cage **2** with *tren* affords cage **3**. In contrast, *tren* is observed to induce disassembly of cage **1** by extracting its constituents Zn^{II} and 2-formylpyridine to form the mononuclear complex zinc(II) tris(pyridyliminoethyl)amine and release free **A** (Figure S86).[36] Remarkably, the outcome of the reaction of a mixture of **1** and **2** with *tren* was observed to be pathway dependent.[15g,37]

The addition of *tren* (4 equiv) to a mixture of **1** and **2** (1:1) in CD_3CN resulted in the selective disassembly of cage **1** (Figure S83). After 10 min at 25 ºC, 60% of **1** had already been consumed whereas **2** remained intact. After equilibration of this mixture at 60 ºC for 12 h, cage **1** had been totally consumed and the mononuclear complex formed (ca. 4 equiv relative to the initial amount of **1**).[38] A decrease in the total amount of cage **2** was also observed (ca. 20% by ^{1}H NMR integration), which we infer to be due to the reaction between liberated **A** and **2** (as discussed below), yet no signals

corresponding to cage **3** or free **A** were identified. Subsequent addition of *tren* (5 equiv) did not result in the expected transformation of **2** into **3**, resulting instead in the formation of insoluble material. Only the mononuclear complex and *p*-toluidine were observed in solution after heating the mixture overnight to 70 ºC. We infer the precipitate to result from the reaction of subcomponents **A** and **B**, which are only sparingly soluble in acetonitrile.[39]

In a separate experiment we also tested the reaction of the mixture of **1** and **2** with excess *tren* (10 equiv: more than the amount required to break down **1** and convert **2** into **3**) in a single addition (Figure S84). The ^{1}H NMR spectrum of the mixture after heating to 70 ºC for 12 h confirmed complete disassembly of **1** accompanied by formation of the mononuclear complex and release of **A**, as well as the formation of cage **3** with release of *p*-toluidine, while no precipitate was observed.

This pathway-dependant reaction outcome may be a consequence of the ability of *tren* to induce the partial disassembly of **2** by first extracting the metal template from the structure. Such extraction has been observed to occur during the substitution reaction with *tren* of Fe^{II}-containing cages,[18] and we infer it to be more favorable in a system based on Zn^{II}, a more labile metal ion. Following the *tren*–mediated partial disassembly of **2**, the free tris-aniline **A** present in the mixture may interfere with the reaction pathway leading ultimately to the formation of **3**. We infer the reaction between tris-aniline **A** and tris-formylpyridine **B** to result in the formation of crosslinked oligomeric material that precipitates, thus removing both subcomponents from solution during the disassembly of cage **2** in the presence of **A**. Indeed, the addition of *tren* (4.5 equiv) to a solution containing **2** and tris-aniline **A** (4.5 equiv) resulted in precipitation (Figure S87) and not the formation of **3**. We thus infer this process to occur on the second addition of *tren* to the cage mixture, once **1** has disassembled. A single addition of the amount of *tren* required to react with both cages in the initial mixture, in contrast, suppresses the formation of insoluble oligomeric material. In this case, we hypothesize that a broader range of more flexible and soluble intermediate products may be generated, in which *tren* has partially reacted with the frameworks of both **1** and **2**. The excess *tren* thus serves as a buffer by preventing **A** and **B** from reacting directly in these intermediate states, thus keeping **B** in solution long enough for **3** to form.

Control of sequential guest release through orthogonal chemical signals. The studies described above enabled us to devise a system displaying complex stimuli-responsive guest release behavior (Scheme 1). Each step of the sequence was monitored by NMR (Figures 5 and S88 – S91).

Starting from a mixture of $C_6H_{12}\subset$**1**, $CHCl_3\subset$**2** and 'empty' **2** (1:0.5:0.5), the sequential addition of *tren* and then ReO_4^- brought about the release of cyclohexane and chloroform in that order, as shown in Sequence I of Scheme 1. *i*) The selective release of cyclohexane upon disassembly of cage **1** occurred following the addition of *tren* (4 equiv relative to the total amount of **1**) and heating at 60 ºC for 12 hours. This process was tracked by following the disappearance of the ^{1}H NMR resonances corresponding to encapsulated cyclohexane and cage **1** (Figure S88). As described in the analogous experiment in the absence of guests, a small amount of cage **2** had also been consumed (ca. 20%) after heating. *ii*) The subsequent addition of ReO_4^- (1.1 equiv) brought about the complete displacement of $CHCl_3$ from **2** to form the $ReO_4^-\subset$**2** inclusion complex after equilibration of the mixture at 70 ºC for 2h. *iii*) Finally, the liberation of ReO_4^- was achieved upon disassembly of **2** and precipitation of subcomponents **A** and **B** on addition of a third signal, *tren* (4 equiv), to the previous mixture and heating at 70 ºC for 12h, as confirmed by ^{1}H NMR.[40]

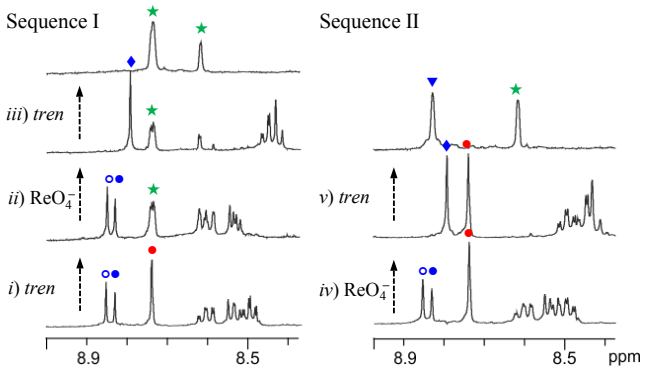

Figure 5. Stacked plots of ^{1}H NMR spectra corresponding to the stimulus/response sequences shown in Scheme 1, starting from a 1:1 mixture of **1** and **2** selectively encapsulating cyclohexane and chloroform, respectively. Only the imine signals of the different species are labeled as follows: ● = $C_6H_{12}\subset$**1**, ○ = 'empty' **2**, ● = $CHCl_3\subset$**2**, ♦ = $ReO_4^-\subset$**2**, ▼ = $ReO_4^-\subset$**3** and ★ = mononuclear complexes. Intensities have been scaled for clarity.

When the sequence of signals applied was reversed, so was the order of guests released, as shown in sequence II in Scheme 1. *iv*) Chloroform was selectively displaced from the cavity of cage **2** following the addition of ReO_4^- (1.6 equiv) to the starting host-guest system and equilibration of the mixture at 70 ºC for 2h, as confirmed by ^{1}H NMR (Figures 5 and S89). *ii*) Addition of *tren* (10 equiv) to the previous mixture triggered disassembly of cage **1**, thus releasing cyclohexane, and the transformation of cage **2** into **3** with concomitant entrapment of ReO_4^- inside the latter. After equilibration of the sample at 70 ºC for 12 h, the ^{1}H NMR spectrum confirmed formation of mononuclear complexes, disappearance of the resonances due to $C_6H_{12}\subset$**1**, formation of $ReO_4^-\subset$**3**, and the presence of free *p*-toluidine and tris-aniline **A** in solution. The mixture remained soluble throughout the experiment.

Chloroform, cyclohexane and perrhenate were used as a representative guest set. Additionally, we have demonstrated the same orthogonal control over the guest release sequence with PF_6^- (in place of $CHCl_3$), cyclohexane and ReO_4^- (see Supporting Information section 5.2). Other mixtures are predicted to behave similarly, as long as the first two guests are chosen to bind selectively within **1** and **2**, and the third guest has a higher affinity for **2** than its initial guest. Alternatively, in keeping with the differential anion affinities of **2** and **3**, anions such as BF_4^-, NO_3^- or ClO_4^-, could be incorporated in place of ReO_4^- in this network, which would result in their release upon transformation of **2** into **3** in step *v)* of Sequence II.

Conclusions

The guest binding properties of two new $Zn^{II}_4L_4$ tetrahedra based on a tris-formylpyridine subcomponent have been studied in detail. The differing reactivity of tris-formylpyridine and tris-aniline based structures with *tren* has also been investigated. The insights gained have enabled the design of a chemical system with complex guest encapsulation behavior, in which three guests are individually released in response to distinct chemical signals. As a result, sequence-selective guest release triggered by the specific order of applied stimuli was demonstrated, while the identification of a pathway-dependent reaction of the cage mixture with *tren* brought about control over the system's overall response, release or capture of the third guest at the end of the sequence.

These findings provide new means for the rational design of more complex systems. Control over the order in which guests are released on demand might be exploited in the development of multi-drug delivery systems, to control the sequential reactivity of multiple catalysts in a reaction mixture, or the release of guests that act as signals to activate subsequent processes. This work thus demonstrates how the study of systems composed of multiple molecular containers with different properties and stimuli-responsive behavior may allow new complex properties and functions, such as pathway-dependent reactivity, to emerge.

Additionally, cage **2** was found to be an outstanding host for perrhenate, which can be permanently trapped by *in situ* transformation into cage **3** by the addition of *tren*. This slow guest exchange kinetics observed for *tren* containing **3** may be relevant for the construction of new more stable capsules for trapping and storage of perrhenate, pertechnetate, or other guests.

ASSOCIATED CONTENT

Supporting Information

General synthetic methods, revised synthesis of **B**, synthesis and characterization of cages **2** and **3**, NMR and ESI-MS spectra, full experimental procedures for the determination of association constants, kinetics of anion uptake studies, selective-sequence guests release experiments and volume calculations and CIF files. This material is available free of charge via the Internet at http://pubs.acs.org. Crystallographic data have also been deposited with the Cambridge Crystallographic Data Centre (entries CCDC 1410005 – 1410007).

AUTHOR INFORMATION

Corresponding Author

jrn34@cam.ac.uk

Notes

The authors declare no competing financial interests.

ACKNOWLEDGMENT

This work was supported by the European Research Council. We thank Diamond Light Source (UK) for synchrotron beamtime on I19 (MT8464) and Dr. Rana A. Bilbeisi for a preliminary screening of guests for cage **1**.

REFERENCES

(1) (a) Ludlow, R. F.; Otto, S. *Chem. Soc. Rev.* **2008**, *37*, 101. (b) Mattia, E.; Otto, S. *Nature Nanotech.* **2015**, *10*, 111. (c) Lehn, J.-M. *Angew. Chem. Int. Ed.* **2013**, *52*, 2836.

(2) (a) del Amo, V.; Philp, D. *Chem. - Eur. J.* **2010**, *16*, 13304. (b) Chung, M.-K.; Severin, K.; Lee, S. J.; Waters, M. L.; Gagne, M. R. *Chem. Sci.* **2011**, *2*, 744. (c) You, L.; Berman, J. S.; Anslyn, E. V. *Nature Chem.* **2011**, *3*, 943. (d) Ritson, D.; Sutherland, J. D. *Nature Chem.* **2012**, *4*, 895. (e) Wilson, A.; Gasparini, G.; Matile, S. *Chem. Soc. Rev.* **2014**, *43*, 1948. (f) Hsu, C.-W.; Miljanić, O. Š. *Angew. Chem. Int. Ed.* **2015**, *54*, 2219. (g) van der Zwaag, D.; de Greef, T. F. A.; Meijer, E. W. *Angew. Chem. Int. Ed.* **2015**, *54*, 2.

(3) (a) de Ruiter, G.; van der Boom, M. E. *Acc. Chem. Res.* **2011**, *44*, 563. (b) Kloxin, C. J.; Bowman, C. N. *Chem. Soc. Rev.* **2013**, *42*, 7161. (c) Hu, J.; Liu, S. *Acc. Chem. Res.* **2014**, *47*, 2084. (d) Isaacs, L. *Acc. Chem. Res.* **2014**, *47*, 2052. (e) Qi, Z.; Schalley, C. A. *Acc. Chem. Res.* **2014**, *47*, 2222. (f) Su, X.; Aprahamian, I. *Chem. Soc. Rev.* **2014**, *43*, 1963. (g) Wojtecki, R. J.; Meador, M. A.; Rowan, S. J. *Nature Mater.* **2011**, *10*, 14. (h) Brioche, J.; Pike, S. J.; Tshepelevitsh, S.; Leito, I.; Morris, G. A.; Webb, S. J.; Clayden, J. *J. Am. Chem. Soc.* **2015**, *137*, 6680.

(4) (a) Gianneschi, N. C.; Nguyen, S. T.; Mirkin, C. A. *J. Am. Chem. Soc.* **2005**, *127*, 1644. (b) Rodríguez-Llansola, F.; Meijer, E. W. *J. Am. Chem. Soc.* **2013**, *135*, 6549. (c) Qian, H.; Aprahamian, I. *Chem. Commun.* **2015**, *51*, 11158.

(5) (a) Shaywitz, A.; Greenberg, M. *Annu. Rev. Biochem.* **1999**, *68*, 821. (b) Barrell, M. J.; Campaña, A. G.; von Delius, M.; Geertsema, E. M.; Leigh, D. A. *Angew. Chem. Int. Ed.* **2011**, *50*, 285. (c) Wang, C.; Li, Z.; Cao, D.; Zhao, Y.-L.; Gaines, J. W.; Bozdemir, O. A.; Ambrogio, M. W.; Frasconi, M.; Botros, Y. Y.; Zink, J. I.; Stoddart, J. F. *Angew. Chem. Int. Ed.* **2012**, *51*, 5460. (d) Tian, F.; Jiao, D.; Biedermann, F.; Scherman, O. A. *Nat. Commun.* **2012**, *3*, 1207. (e) Xiao, W.; Zeng, X.; Lin, H.; Han, K.; Jia, H.-Z.; Zhang, X.-Z. *Chem. Commun.* **2015**, *51*, 1475.

(6) (a) Chen, S.; Itoh, Y.; Masuda, T.; Shimizu, S.; Zhao, J.; Ma, J.; Nakamura, S.; Okuro, K.; Noguchi, H.; Uosaki, K.; Aida, T. *Science* **2015**, *348*, 555. (b) Fukino, T.; Joo, H.; Hisada, Y.; Obana, M.; Yamagishi, H.; Hikima, T.; Takata, M.; Fujita, N.; Aida, T. *Science* **2014**, *344*, 499. (c) Matson, J. B.; Navon, Y.; Bitton, R.; Stupp, S. I. *ACS Macro Letters* **2015**, *4*, 43.

(7) For selected reviews see: (a) Chakrabarty, R.; Mukherjee, P. S.; Stang, P. J. *Chem. Rev.* **2011**, *111*, 6810. (b) Ward, M. D. *Chem. Commun.* **2009**, 4487. (c) Jin, P.; Dalgarno, S. J.; Atwood, J. L. *Coord. Chem. Rev.* **2010**, *254*, 1760. (d) Harris, K.; Fujita, D.; Fujita, M. *Chem. Commun.* **2013**, *49*, 6703. (e) Ronson, T. K.; Zarra, S.; Black, S. P.; Nitschke, J. R. *Chem. Commun.* **2013**, *49*, 2476. (f) Han, M.; Engelhard, D. M.; Clever, G. H. *Chem. Soc. Rev.* **2014**, *43*, 1848. (g) Mukherjee, S.; Mukherjee, P. S. *Chem. Commun.* **2014**, *50*, 2239.

(8) For selected recent examples see: (a) Custelcean, R.; Bonnesen, P. V.; Duncan, N. C.; Zhang, X.; Watson, L. A.; Van Berkel, G.; Parson, W. B.; Hay, B. P. *J. Am. Chem. Soc.* **2012**, *134*, 8525. (b) Pasquale, S.; Sattin, S.; Escudero-Adán, E. C.; Martínez-Belmonte, M.; de Mendoza, J. *Nat. Commun.* **2012**, *3*, 785. (c) Gütz, C.; Hovorka, R.; Klein, C.; Jiang, Q.-Q.; Bannwarth, C.; Engeser, M.; Schmuck, C.; Assenmacher, W.; Mader, W.; Topić, F.; Rissanen, K.; Grimme, S.; Lützen, A. *Angew. Chem. Int. Ed.* **2014**, *53*, 1693. (d) Metherell, A. J.; Ward, M. D. *Chem. Commun.* **2014**, *50*, 10979. (e) Young, M. C.; Holloway, L. R.; Johnson, A. M.; Hooley, R. J. *Angew. Chem. Int. Ed.* **2014**, *53*, 9832. (f) Ramsay, W. J.; Szczypiński, F. T.; Weissman, H.; Ronson, T. K.; Smulders, M. M. J.; Rybtchinski, B.; Nitschke, J. R. *Angew. Chem. Int. Ed.* **2015**, *54*, 5636. (g) Thorp-Greenwood, F. L.; Kulak, A. N.; Hardie, M. J. *Nature Chem.* **2015**, *7*, 526. (h) Wise, M. D.; Holstein, J. J.; Pattison, P.; Besnard, C.; Solari, E.; Scopelliti, R.; Bricogne, G.; Severin, K. *Chem. Sci.* **2015**, *6*, 1004.

(9) (a) Cook, T. R.; Vajpayee, V.; Lee, M. H.; Stang, P. J.; Chi, K.-W. *Acc. Chem. Res.* **2013**, *46*, 2464. (b) Croue, V.; Goeb, S.; Salle, M. *Chem. Commun.* **2015**, *51*, 7275. (c) Therrien, B. *Chem. - Eur. J.* **2013**, *19*, 8378. (d) Ward, M. D.; Raithby, P. R. *Chem. Soc. Rev.* **2013**, *42*, 1619. (e) Xu, L.; Wang, Y.-X.; Yang, H.-B. *Dalton. Trans.* **2015**, *44*, 867. (f) Yoshizawa, M.; Klosterman, J. K.; Fujita, M. *Angew. Chem. Int. Ed.* **2009**, *48*, 3418. (g) Brown, C. J.; Toste, F. D.; Bergman, R. G.; Raymond, K. N. *Chem. Rev.* **2015**, *115*, 3012.

(10) (a) Hristova, Y. R.; Smulders, M. M. J.; Clegg, J. K.; Breiner, B.; Nitschke, J. R. *Chem. Sci.* **2011**, *2*, 638. (b) Neelakandan, P. P.; Jiménez, A.; Nitschke, J. R. *Chem. Sci.* **2014**, *5*, 908. (c) Ronson, T. K.; League, A. B.; Gagliardi, L.; Cramer, C. J.; Nitschke, J. R. *J. Am. Chem. Soc.* **2014**, *136*, 15615. (d) Turega, S.; Whitehead, M.; Hall, B. R.; Meijer, A. J. H.

M.; Hunter, C. A.; Ward, M. D. *Inorg. Chem.* **2013**, *52*, 1122. (e) Yazaki, K.; Kishi, N.; Akita, M.; Yoshizawa, M. *Chem. Commun.* **2013**, *49*, 1630. (f) García-Simón, C.; Garcia-Borràs, M.; Gómez, L.; Garcia-Bosch, I.; Osuna, S.; Swart, M.; Luis, J. M.; Rovira, C.; Almeida, M.; Imaz, I.; Maspoch, D.; Costas, M.; Ribas, X. *Chem. - Eur. J.* **2013**, *19*, 1445. (g) García-Simón, C.; Garcia-Borràs, M.; Gómez, L.; Parella, T.; Osuna, S.; Juanhuix, J.; Imaz, I.; Maspoch, D.; Costas, M.; Ribas, X. *Nat. Commun.* **2014**, *5*, 5557. (h) Frischmann, P. D.; Kunz, V.; Würthner, F. *Angew. Chem.* **2015**, *127*, 7393. (i) Takezawa, H.; Akiba, S.; Murase, T.; Fujita, M. *J. Am. Chem. Soc.* **2015**, *137*, 7043.

(11) (a) Duriska, M. B.; Neville, S. M.; Lu, J.; Iremonger, S. S.; Boas, J. F.; Kepert, C. J.; Batten, S. R. *Angew. Chem. Int. Ed.* **2009**, *48*, 8919. (b) Riddell, I. A.; Smulders, M. M. J.; Clegg, J. K.; Nitschke, J. R. *Chem. Commun.* **2011**, *47*, 457.

(12) (a) Horiuchi, S.; Murase, T.; Fujita, M. *J. Am. Chem. Soc.* **2011**, *133*, 12445. (b) Nakabayashi, K.; Kawano, M.; Fujita, M. *Angew. Chem. Int. Ed.* **2005**, *44*, 5322. (c) Yoshizawa, M.; Kusukawa, T.; Fujita, M.; Yamaguchi, K. *J. Am. Chem. Soc.* **2000**, *122*, 6311.

(13) (a) Hastings, C. J.; Pluth, M. D.; Bergman, R. G.; Raymond, K. N. *J. Am. Chem. Soc.* **2010**, *132*, 6938. (b) Jiao, Y.; Wang, J.; Wu, P.; Zhao, L.; He, C.; Zhang, J.; Duan, C. *Chem. - Eur. J.* **2014**, *20*, 2224. (c) Murase, T.; Horiuchi, S.; Fujita, M. *J. Am. Chem. Soc.* **2010**, *132*, 2866. (d) Otte, M.; Kuijpers, P. F.; Troeppner, O.; Ivanović-Burmazović, I.; Reek, J. N. H.; de Bruin, B. *Chem. - Eur. J.* **2013**, *19*, 10170. (e) Samanta, D.; Mukherjee, S.; Patil, Y. P.; Mukherjee, P. S. *Chem. - Eur. J.* **2012**, *18*, 12322. (f) García-Simón, C.; Gramage-Doria, R.; Raoufmoghaddam, S.; Parella, T.; Costas, M.; Ribas, X.; Reek, J. N. H. *J. Am. Chem. Soc.* **2015**, *137*, 2680.

(14) (a) Zarra, S.; Wood, D. M.; Roberts, D. A.; Nitschke, J. R. *Chem. Soc. Rev.* **2015**, *44*, 419. (b) Northrop, B. H.; Zheng, Y.-R.; Chi, K.-W.; Stang, P. J. *Acc. Chem. Res.* **2009**, *42*, 1554. (c) Meyer-Eppler, G.; Topić, F.; Schnakenburg, G.; Rissanen, K.; Lützen, A. *Eur. J. Inorg. Chem.* **2014**, *2014*, 2495. (d) Niess, F.; Duplan, V.; Sauvage, J.-P. *J. Am. Chem. Soc.* **2014**, *136*, 5876. (e) Johnson, A. M.; Wiley, C. A.; Young, M. C.; Zhang, X.; Lyon, Y.; Julian, R. R.; Hooley, R. J. *Angew. Chem. Int. Ed.* **2015**, *54*, 5641.

(15) (a) McConnell, A. J.; Wood, C. S.; Neelakandan, P. P.; Nitschke, J. R. *Chem. Rev.* **2015**, *115*, 7729. (b) Clegg, J. K.; Cremers, J.; Hogben, A. J.; Breiner, B.; Smulders, M. M. J.; Thoburn, J. D.; Nitschke, J. R. *Chem. Sci.* **2013**, *4*, 68. (c) Han, M.; Michel, R.; He, B.; Chen, Y.-S.; Stalke, D.; John, M.; Clever, G. H. *Angew. Chem. Int. Ed.* **2013**, *52*, 1319. (d) Meng, W.; Ronson, T. K.; Clegg, J. K.; Nitschke, J. R. *Angew. Chem. Int. Ed.* **2013**, *52*, 1017. (e) Sørensen, A.; Castilla, A. M.; Ronson, T. K.; Pittelkow, M.; Nitschke, J. R. *Angew. Chem. Int. Ed.* **2013**, *52*, 11273. (f) Bradberry, S. J.; Savyasachi, A. J.; Martinez-Calvo, M.; Gunnlaugsson, T. *Coord. Chem. Rev.* **2014**, *273–274*, 226. (g) Riddell, I. A.; Ronson, T. K.; Clegg, J. K.; Wood, C. S.; Bilbeisi, R. A.; Nitschke, J. R. *J. Am. Chem. Soc.* **2014**, *136*, 9491.

(16) (a) Smulders, M. M. J.; Zarra, S.; Nitschke, J. R. *J. Am. Chem. Soc.* **2013**, *135*, 7039. (b) Ma, S.; Smulders, M. M. J.; Hristova, Y. R.; Clegg, J. K.; Ronson, T. K.; Zarra, S.; Nitschke, J. R. *J. Am. Chem. Soc.* **2013**, *135*, 5678. (c) Jiménez, A.; Bilbeisi, R. A.; Ronson, T. K.; Zarra, S.; Woodhead, C.; Nitschke, J. R. *Angew. Chem. Int. Ed.* **2014**, *53*, 4556. (d) Cullen, W.; Thomas, K. A.; Hunter, C. A.; Ward, M. D. *Chem. Sci.* **2015**, *6*, 4025. (e) Cullen, W.; Turega, S.; Hunter, C. A.; Ward, M. D. *Chem. Sci.* **2015**, *6*, 625.

(17) (a) Bilbeisi, R. A.; Clegg, J. K.; Elgrishi, N.; de Hatten, X.; Devillard, M.; Breiner, B.; Mal, P.; Nitschke, J. R. *J. Am. Chem. Soc.* **2011**, *134*, 5110. (b) Caulder, D. L.; Brückner, C.; Powers, R. E.; König, S.; Parac, T. N.; Leary, J. A.; Raymond, K. N. *J. Am. Chem. Soc.* **2001**, *123*, 8923. (c) Granzhan, A.; Riis-Johannessen, T.; Scopelliti, R.; Severin, K. *Angew. Chem. Int. Ed.* **2010**, *49*, 5515. (d) Saalfrank, R. W.; Glaser, H.; Demleitner, B.; Hampel, F.; Chowdhry, M. M.; Schünemann, V.; Trautwein, A. X.; Vaughan, G. B. M.; Yeh, R.; Davis, A. V.; Raymond, K. N. *Chem. - Eur. J.* **2002**, *8*, 493. (e) Albrecht, M.; Shang, Y.; Rhyssen, T.; Stubenrauch, J.; Winkler, H. D. F.; Schalley, C. A. *Eur. J. Org. Chem.* **2012**, *2012*, 2422.

(18) Castilla, A. M.; Ousaka, N.; Bilbeisi, R. A.; Valeri, E.; Ronson, T. K.; Nitschke, J. R. *J. Am. Chem. Soc.* **2013**, *135*, 17999.

(19) Katayev, E. A.; Kolesnikov, G. V.; Sessler, J. L. *Chem. Soc. Rev.* **2009**, *38*, 1572, and references therein.

(20) Busschaert, N.; Caltagirone, C.; Van Rossom, W.; Gale, P. A. *Chem. Rev.* **2015**, *115*, 8038.

(21) (a) Kolesnikov, G. V.; German, K. E.; Kirakosyan, G.; Tananaev, I. G.; Ustynyuk, Y. A.; Khrustalev, V. N.; Katayev, E. A. *Org. Biomol. Chem.* **2011**, *9*, 7358. (b) Rambo, B. M.; Sessler, J. L. *Chem. - Eur. J.* **2011**, *17*, 4946. (c) Cao, R.; McCarthy, B. D.; Lippard, S. J. *Inorg. Chem.* **2011**, *50*, 9499. (d) Alberto, R.; Bergamaschi, G.; Braband, H.; Fox, T.; Amendola, V. *Angew. Chem. Int. Ed.* **2012**, *51*, 9772. (e) Freye, S.; Michel, R.; Stalke, D.; Pawliczek, M.; Frauendorf, H.; Clever, G. H. *J. Am. Chem. Soc.* **2013**, *135*, 8476. (f) Kataev, E. A.; Pantos, P.; Karnas, E.; Kolesnikov, G. V.; Tananaev, I. G.; Lynch, V. M.; Sessler, J. L. *Supramol. Chem.* **2014**, *27*, 346. (f) Lim, J. Y. C.; Beer, P. D. *Chem. Commun.* **2015**, *51*, 3686.

(22) (a) Custelcean, R. *Chem. Soc. Rev.* **2014**, *43*, 1813. (b) Pluth, M. D.; Raymond, K. N. *Chem. Soc. Rev.* **2007**, *36*, 161.

(23) Kleywegt, G. J.; Jones, T. A. *Acta Cryst.* **1994**, *D50*, 178.

(24) Mecozzi, S.; Rebek, J. J. *Chem. - Eur. J.* **1998**, *4*, 1016.

(25) Charged hosts have previously been observed not to obey Rebek's 55% optimal-occupancy "rule". See references 8f, 15b and 22a.

(26) Chifotides, H. T.; Dunbar, K. R. *Acc. Chem. Res.* **2013**, *46*, 894.

(27) *Anion Coordination Chemistry*; Wiley-VCH: Weinheim, 2011.

(28) Moyer, B. A.; Custelcean, R.; Hay, B. P.; Sessler, J. L.; Bowman-James, K.; Day, V. W.; Kang, S.-O. *Inorg. Chem.* **2013**, *52*, 3473.

(29) See Figure S97 in the Supporting Information for an overlay of the structures **2** and **3** in the solid state.

(30) Some association in solution between polycationic hosts and anions has been previously described, see for instance: Frantz, R.; Grange, C. S.; Al-Rasbi, N. K.; Ward, M. D.; Lacour, J. *Chem. Commun.* **2007**, 1459.

(31) Sanders, J. K. M.; Hunter, B. K. *Modern NMR Spectroscopy: A Guide for Chemists*; Oxford University Press: Oxford, UK, 1993.

(32) Pastor, A.; Martínez-Viviente, E. *Coord. Chem. Rev.* **2008**, *252*, 2314.

(33) Exchange spectroscopy (2D EXSY) has been applied for studying kinetics of reversible systems that exchange slowly on the chemical shift timescale but fast in the spin-lattice (T_1) relaxation timescale. In practice, exchange processes with rates rate constants between 10^2 and 10^{-2} s^{-1} can be investigated. For selected examples see references 10d and 16a-b.

(34) Although Zn^{II} is a labile metal ion it has been shown that tightly interlocked structures, like these $Zn^{II}_4L_4$ assemblies with rigid ligands, provide largely increased kinetic stabilities. See: (a) Charbonnière, L. J.; Williams, A. F.; Frey, U.; Merbach, A. E.; Kamalaprija, P.; Schaad, O. *J. Am. Chem. Soc.* **1997**, *119*, 2488. (b) Paul, R. L.; Bell, Z. R.; Jeffery, J. C.; Harding, L. P.; McCleverty, J. A.; Ward, M. D. *Polyhedron* **2003**, *22*, 781.

(35) (a) Davis, A. V.; Raymond, K. N. *J. Am. Chem. Soc.* **2005**, *127*, 7912. (b) Davis, A. V.; Fiedler, D.; Seeber, G.; Zahl, A.; van Eldik, R.; Raymond, K. N. *J. Am. Chem. Soc.* **2006**, *128*, 1324.

(36) Mal, P.; Schultz, D.; Beyeh, K.; Rissanen, K.; Nitschke, J. R. *Angew. Chem. Int. Ed.* **2008**, *47*, 8297.

(37) Chepelin, O.; Ujma, J.; Barran, P. E.; Lusby, P. J. *Angew. Chem. Int. Ed.* **2012**, *51*, 4194.

(38) Formation of two different Zn^{II} mononuclear complexes was observed by ^{1}H NMR: the octahedral complex zinc(II) tris(pyridyliminoethyl)amine (Scheme 1) and a zinc(II) trigonal bipyramidal complex where the ligand is formed from the condensation of *tren* with only 1 equiv of 2-formylpyridine. See Figure S85 in the Supporting Information for details.

(39) **B** is insoluble in acetonitrile whereas **A** is soluble enough to be observed by ^{1}H NMR at the concentrations used in this work. In experiments not resulting in precipitation, NMR signals due to free **A** were observed with integrals matching the concentration of **1** in the initial mixture.

(40) Formation of the complex $ReO_4^-\subset$**2** was observed upon addition of **2**•$[NTf_2]_8$ to the final reaction mixture generated from sequence I (after removal of the precipitate by filtration), thus confirming ReO_4^- remains in solution. See Figures S88 and S91 in the Supporting Information.

TOC graphic